FIFTH AUSTRALASIAN CONFERENCE

on

HYDRAULICS AND FLUID MECHANICS

at

University of Canterbury, Christchurch, New Zealand

1974 December 9 to December 13

ARTIFICIAL BOUNDARIES FOR MODELS OF FREE CONVECTION

by

R. A. Pearson, J. L. McGregor and B. R. Morton

SUMMARY

Numerical models of free convection usually introduce a small closed box, inside of which the convection occurs. The effects of this spurious boundary are discussed. A number of simple boundary conditions that allow inflow and outflow through the boundaries are devised. The results of computations using different sized boxes and different boundary conditions are compared.

R. A. Pearson, Monash University.
J. L. McGregor, Monash University.
B. R. Morton, Monash University.
This work was supported by an A.R.G.C. Grant.

1. INTRODUCTION

Two and three dimensional numerical models of clouds usually assume that the flow is generated by a parcel, or bubble, of hot or humid air present in the atmosphere. The surrounding air is usually at rest although an overall shear flow may be introduced. The equations of motion are then numerically integrated and the development of the cloud is followed, (.e.g Lilly 1962, Ogura 1963, Daley & Merilees 1972, Clark 1973). The flow, without precipitation, is similar to that of laboratory models (e.g. Richards 1963) in the laboratory, as in the atmosphere, the bubble of hot air, and the corresponding flow is much smaller than the "container". However, in the numerical model the restrictions of computer size and time require a box that is not much larger than the parcel of air and its flow (e.g. fig. 1).

In cloud modelling the computational box is usually assumed to have rigid sides, (e.g. Song & Ogura 1973). Lilly (1964) uses a moving co-ordinate system, he estimates a-posteriori the change in streamline pattern, at steady state that could be expected if an open boundary was used. This does not show any possible influence of the boundaries on the development of the flow.

The usual boundary condition on the temperature field is that the box has insulating sides. In a spatially fixed model the hot air will eventually h t and move along the top (fig. 1). All boundaries also have a free slip condition imposed.

In other fields of numerical modelling attempts have been made to allow flow through boundaries. Flow through the boundaries of a mesoscale model of the atmosphere was allowed by Shapiro & O'Brien (1970). While the boundary condition for surface gravity waves on the ocean were used by Vastano & Reid (1967), and by Wurtele et al (1971). The gravity wave problem, for a dispersive system was discussed by Pearson (1973, 1974). Flow through the side boundaries of a heat island was allowed by Leslie and Morton (1973).

The appropriate boundary condition for cloud models will probably depend on the ambient conditions. This paper considers only a neutral environment. In a stably stratified case internal gravity waves may be important and the Summerfield Radiation Boundary Condition could be used (e.g. Pearson 1974).

2. THE BASIC MODEL

The initial perturbation, and all subsequent flow is to be two dimensional, with flow in the X-Z plane. The air is dry, and the Boussinesq approximation is assumed to be valid. With the introduction of a streamfunction χ ; where $u = \frac{\partial \chi}{\partial z}$, $w = \frac{\partial \chi}{\partial X}$, $\zeta = \frac{\partial u}{\partial z} - \frac{\partial u}{\partial X} = \nabla^2 \chi$;

the equations of motion can be written as

$$\frac{\partial \zeta}{\partial t} = J(\chi,\zeta) - \beta g \frac{\partial \theta}{\partial X} + \nu \nabla^2 \zeta$$

$$\frac{\partial \theta}{\partial z} = J(\chi,T) + K\nabla^2\theta.$$

For the affects of turbulence a constant coefficient of Eddy Viscosity has been used. However, a variable form (Lilly 1963) could also be used.

The fluid is initially at rest with a temperature perturbation symmetric about X=0. This perturbation is of the same form as that of Soong & Ogura (1973).

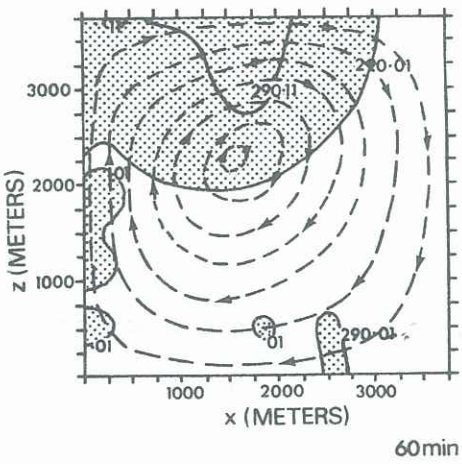

Figure 1 Stream function and temperature field, according to Lilly (1962).

$$T(x,z) = T_o + T_e\,[1 - (\frac{x}{x_d})^2)(1 - (\frac{z-z_m}{z_d})^2] \quad -x_d \leq x \leq x_d$$

$$z_d - z_m \leq x \leq zd + z_m$$

$$= T_o. \qquad \text{otherwise.}$$

From symmetry $(\frac{\partial T}{\partial x}=0)$ at $x=0$ we have $\chi=0$, and $\zeta=0$. At $z=0$ a rigid $(\chi=0)$ free slip $(\zeta=0)$ insulating $(\frac{\partial T}{\partial z}=0)$ boundary will be used. However, a similar technique considered in this in this paper at only the top and side boundary could be used at $z=0$.

The further restriction of $\nu=K$ is introduced so that the pseudo Rayleigh number for the flow will be given by

$$R = \frac{\beta g}{K^2} \iint [(T(x,z) - T_o]dx\,dz.$$

3. NUMERICAL METHOD

The temperature, vorticity and stream function are defined at the same grid points $(j\Delta x, k\Delta z)$. Second order centred finite difference methods are used for the linear terms. The non-linear terms in the equations are represented by Arakawa's Jacobian (1966). This is a quadratically conservative finite difference scheme. This gives poor phase errors in the advective terms (Orzag 1971). A staggered grid (e.g. Pearson 1973) has twice the accuracy. However, the model was initially developed for comparison with a more extensive modelling of the turbulence and turbulent transfer (Morton 1969). This more complicated form did not seem natural on a staggered grid.

The Nyström (or "leap frog") technique is applied to the time integration, where for stability the diffusion terms are evaluated at the lagged time step. The linear stability of the diffusion terms requires

$$\Delta t < \frac{\Delta x^2}{16K} \quad \text{if} \quad \Delta x = \Delta z.$$

4. GENERAL BEHAVIOUR

As in previous boundary conditions the type of flow generated by a model without boundaries will help in determining the appropriate value of the fields at the boundary. The general behaviour of the flow is now described.

Initially there is no vorticity inside the fluid. The temperature gradients will generate vorticity. As the temperature field is symmetric about the axis $x=0$ the vorticity is skew symmetric. The corresponding flow field advects the overall temperature excess upwards. The maximum value of the temperature perturbation is decreased by the conduction of heat. This spreads the temperature field over a larger area of fluid. The vorticity is similarly affected by the viscosity, while at the axis $x=0$ vorticity is dissipated.

An analytic continuation of the field below the rigid bottom boundary $(z=0)$ gives an image temperature vorticity, and flow field. This image has the negative vorticity of the upper one, with negative gravity. The total vorticity occurs as a "quadrupole".

5. DERIVATION OF THE BOUNDARY CONDITION

The stream function field for a single vortex pair of strength ω_i spread over an area ΔA with centre $(\pm x_i, z_i)$ is given by

$$\chi(x,z) = \frac{\omega_i}{4\pi}\,\Delta A\,\log[\frac{(x-x_i)^2+(z-z_i)^2}{(x+x_i)^2+(z-z_i)^2}] \qquad (5.1)$$

(e.g. Lamb 1879).

For a number of vortex pairs the stream function field can be obtained by summing the contributions for all vortex pairs in the system.

In the present model every grid point $j\Delta x$, $k\Delta x$ with vorticity ζ_{jk} is assumed to be part of such a vortex pair. With the bottom rigid boundary, or image vorticity below the axis

we have

$$\chi(x,z) = \sum_j \sum_k \frac{\zeta_{jk}\Delta x\,\Delta z}{4\pi} \log\left[\frac{(x-x_j)^2+(z-z_k)^2}{(x+x_j)^2+(z-z_k)^2}\right]\left[\frac{(x-x_j)^2+(z+z_k)^2}{(x+x_j)^2+(z+z_k)^2}\right] \quad . \tag{5.2}$$

If all the vorticity is confined to the region $j\Delta x < N\Delta X$; $k\Delta z < M\Delta Z$ then the stream function field at the boundary points can be found from the double sum above taken over $j<N$, $k<M$.

This, however, will require a double sum for each point on the boundary, and hence a large amount of computer time. A number of simplifications are therefore introduced.

(a) Consider polar co-ordinates (r,ϕ) that coincide with the previous (x,z) co-ordinate system. Then from Kellog (1924) we have for $r>r_i$

$$-\frac{1}{2}[\log[(x-x_i)+(z-z_i)^2] = \log\frac{1}{r} + \cos(\phi-\phi_i)\frac{r_i}{r} + \frac{1}{2}\cos 2(\phi-\phi_i)\frac{r_i}{r^2} + \frac{1}{3}\cos 3(\phi-\phi_i)\frac{r^3}{r_i^3} \quad . \tag{5.3}$$

Substituting (5.3) and a similar expansion for $x+x_i$ into (5.1) we have

$$\chi(x,z) = \frac{-\omega_i dA}{\pi}\{\cos\phi\cos\phi_i\frac{r_i}{r} + \frac{1}{2}\sin\phi\sin\phi_i\frac{r_i^2}{r^2} + \frac{1}{3}\cos 3\phi\cos 3\phi_i\frac{r_i^3}{r^3} + \ldots\ldots\} \tag{5.4}$$

In the cartesian co-ordinate system for the upper vortex pair

$$\chi_{jk}(x,z) = -\frac{x_j\zeta_{jk}\Delta x\Delta z}{\pi r^2}\left(1 + \frac{2zz_k}{r^2} + \frac{1}{3r^4}(x^2-3z^2)(x_i^2-3z_k^2) + \frac{4zz_k}{r^6}(x^2-z^2)(x_j^2-z_k^2)\right.$$
$$\left. + \frac{1}{5r^8}(x^4-10x^2z^2+5z^4)(x_j^2-10x_j^2z_k^2+5z^4) \quad + \right. \tag{5.5}$$

As many terms as necessary can be used in this expansion. However, it is valid for $r>r$ and in the terms used above contains errors of $(\frac{r_i}{r})^4$. The advantage of this expansion is that when this expansion is substituted into (5.2) the sum of each of the moments over all points within the domain of integration need only be done once.

(b) Far from the centres of vorticity the stream function pattern will resemble that of a line vortex centred at some point $(\bar{x},\bar{z})$. The traditional definition (Lamb 1879) gives

$$\bar{x} = \frac{\sum\sum x_i\,\zeta_{ij}\,\Delta x\Delta z}{\sum\sum \zeta_{ij}\,\Delta x\Delta z} \tag{5.6}$$

$$\bar{z} = \frac{\sum\sum z_j\,\zeta_{ij}\,\Delta x\Delta z}{\sum\sum \zeta_{ij}\,\Delta x\Delta z} \tag{5.7}$$

where circulation is given by

$$\bar{\omega} = \sum\sum \zeta_{ij}\,\Delta x\Delta y \quad . \tag{5.8}$$

When all the velocity is considered substituting into (5.2) gives

$$\chi(x,y) = \frac{\bar{\omega}}{4}\log\left[\frac{(x-\bar{x})^2+(z-\bar{z})^2}{(x+\bar{x})^2+(z-\bar{z})^2}\right]\left[\frac{(x-\bar{x})^2+(z+\bar{z})^2}{(x+\bar{x})^2+(z+\bar{z})^2}\right] \quad . \tag{5.9}$$

(c) The first term of (5.5) suggests the mean height of the vortex could be defined by

$$\bar{z} = \frac{\sum\sum x_i\,z_j\,\zeta_{ij}\,\Delta x\Delta z}{\sum\sum x_i\,\zeta_{ij}\,\Delta x\Delta z} \quad . \tag{5.10}$$

(d) In (5.3) the polar co-ordinate system has been centred at the origin. However, better convergence will occur for larger r. The r_i can be minimised by setting the centre of the co-ordinate system for the vortex pair above the axis at $(x,\bar{z})$ and setting the distances r,x relative to this centre. The lower system is then centred at $(0,-\bar{z})$. The contributions from

both are then added to obtain the total field.

6. CONSISTENCY OF THE BOUNDARY CONDITIONS

The definition of the stream function along the boundaries by this derived condition will, in general, allow flow through the boundaries.

The values of the temperature and vorticity at this boundary must also be specified in such a manner that this flow does not advect into the computational region spurious heat or vorticity. If a gradient condition is used the finite difference analoge will actually specify the value at the boundary. For example if $\frac{\partial T}{\partial z} = 0$ at $z = H$ then a first order approximation is $x = H$

$x = H - \Delta x$.

If outflow is occurring at the edge the specification of the temperature or vorticity at the boundary may be inconsistent with the interior flow. Assume that the condition $\zeta = 0$ is applied at $z = H$. If $\zeta\big|_{z=H-\Delta z, t=\tau}$ is non-zero the advection would, at some later time, give $\zeta\big|_{z=H, t=\tau'}$ to be non-zero. This is in contradiction to the applied boundary condition.

In deriving the boundary condition it has been assumed that there is no vorticity outside the computational box. As a temperature gradient will generate vorticity this requires that there is no temperature perturbation outside this domain. The hot air inside the box rises, and may reach one grid point inside the top boundary. In a larger box it could continue to rise generating vorticity. The boundary condition is therefore only valid until the temperature perturbation reaches the top of the box. If at $z = H = \Delta z$ the temperature perturbation is non-zero the use of a gradient condition $Hz - z = H$ will force a non-zero temperature perturbation at $z = H$. If inflow is occurring this heat will be advected into the computational region. Similarly, vorticity may be advected into the region. This advection will not, in general, be that which would occur if the region was extended.

To satisfy all these requirements the boundary conditions will be consistent while the vorticity and temperature perturbations remain completely inside a box of size $H - \Delta z$, $L - \Delta x$.

RESULTS

The first comparison discussed has an initial maximum temperature of 1°C and an eddy viscosity of $50 m^2 sec^{-1}$. Other relevant parameters are $\Delta x = 100$ m, $\Delta z = 100$ m, $\Delta t = 10$ sec, $x_d = 1$ kilometer, $z_d = 400$ metres, $z_m = 39$ metres. This gives a pseudo Rayleigh number of 3.77

The flow field was then obtained in a computational box of 9.6 kms by 6.4 kms with the most simplified boundary condition equation (5.9). A small box of 4 km by 3.3 km was also used with rigid sides and boundary condition (5.9). While an intermediate box of 4.8 by 3.3 km using a rigid boundaries, and the boundary conditions of (5.2) and the simplifications (b) and (d). Simplification (c) was not used as it was found that in all previous experiments the mean height for this vortex as defined by (c) was not significantly different from that of (b). The developing and developed vortex (figure 2) has, however, a simple compact form. In the experiment the vortex rose to the top of the computational box. The series expansions (a) and (d) eventually becomes obviously invalid, at which time the computation is ceased, while the height and distance from the axis at which they occur differs. This variation is shown also in the centre of the vortex (figure). The affect of the lid is clearly shown to retard the advance of the vortex which then moves along the top of the box. The rigid lid will also effect the maxima and minima velocities that are predicted by the model. Significantly decreasing the maximum vertical velocity. The fields predicted by all versions of the boundary conditions are very close to those of the larger box until the vortex reaches the top of the box (54 minutes).

CONCLUSION

As all of the derived conditions simulate an unbounded domain effectively until the thermal reaches the top of the computational region. The simplest, and quickest version based on the average centre of the vortex has sufficient accuracy for general use.

REFERENCES

Arakawa, A. (1966) Journal Comp. Physics, 1(1) , 119 - 143.
Clark, T. L. (1973) J.A.S., 30(5) , 857 - 878.
Kellog, O. D. (1924) "Foundations of Potential Theory".
Ogura, Y. (1962) J.A.S., 19 , 493 - 502.
Orzag, (1971) J.F.M., 49(1) , 75 - 112.
Shapiro, M. A. and O'Brien, J. J. (1970) J.Appl.Met., 9 , 345 - 349.
Soong, S. T. and Ogura, Y. (1973) J.A.S., 30(5) , 879 - 893.
Vastano, A. C. and Reid, R. O. (1967) Journal Mar.Res., 129 - 131.

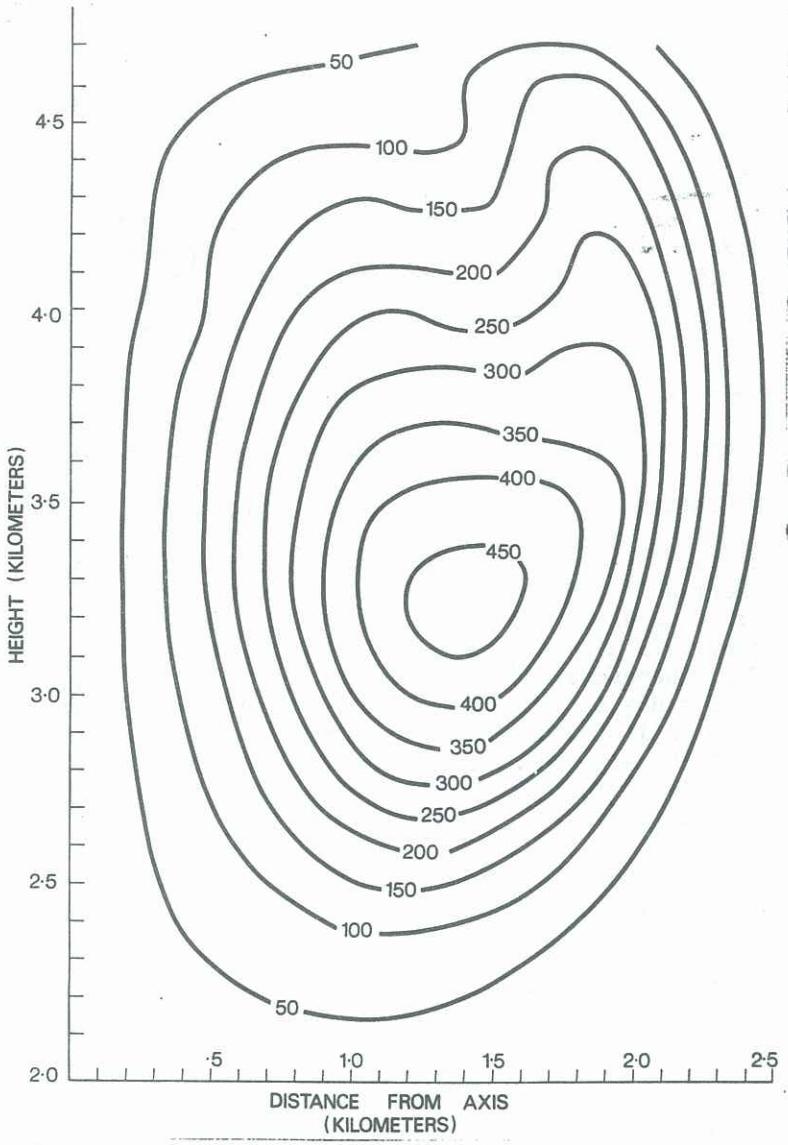

Figure 2 (top left) vorticity pattern at 60 minutes with the simplest open boundary on a box 4.8 by 3.3 kms.

Figure 3 (bottom left) total circulation in box of 4.7 by 3.2 kms.

- total box 4.6 × 6.4 kms;
- equation (5.2) in a box of size 4.8 × 3.3 kms;
- expansion from variation (d) of equation (5.5);
- boundary conditions based on mean centre equation (5.9);
- rigid boundaries on a box of 4.8 × 3.3 kms;
- rigid boundaries on a box of 4.0 × 3.3 kms;
- boundary conditions based on mean vortex centre equation (5.9) in a box 4.0 × 3.3 kms.

Figure 4 (bottom right) height of the mean centre of the vortex (code as for figure 3).

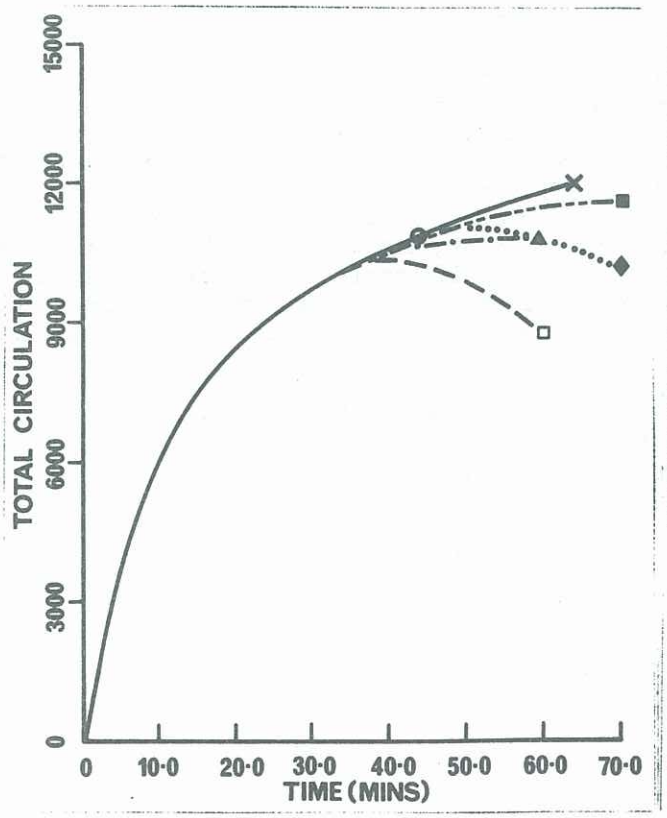

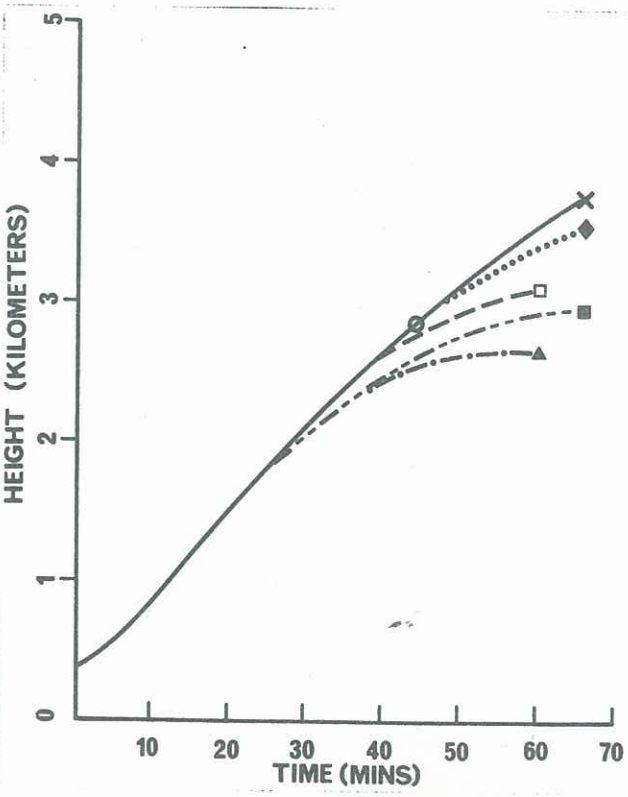

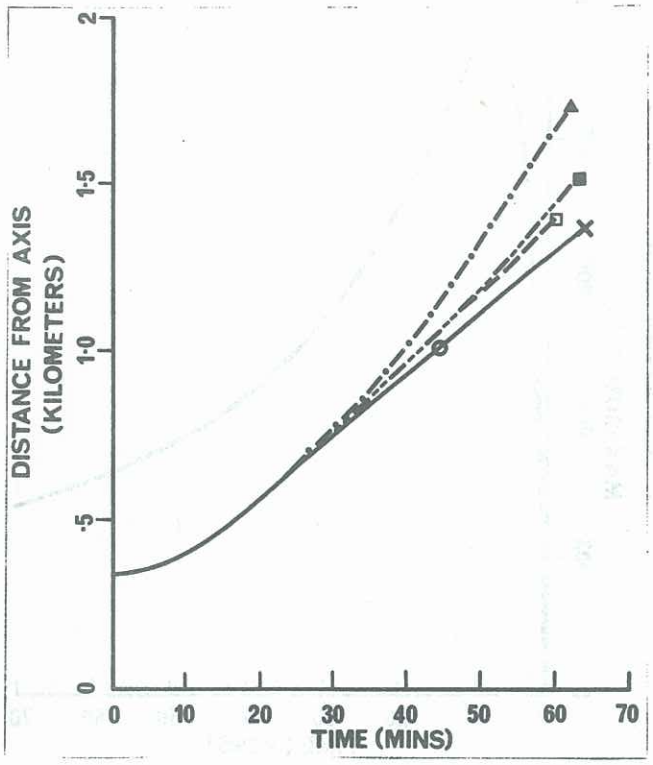

Figure 5: radius of the mean centre, code as for figure 3.

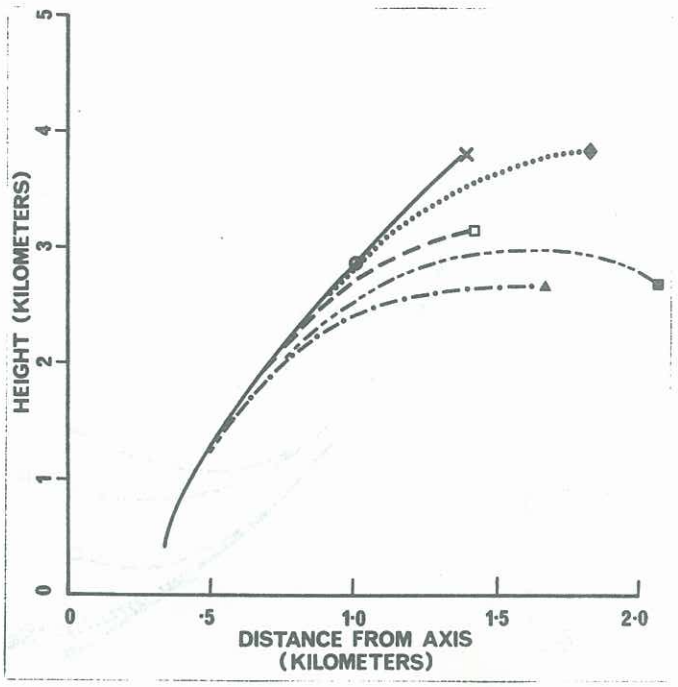

Figure 6: path of the centre of circulation, code as for figure 3.

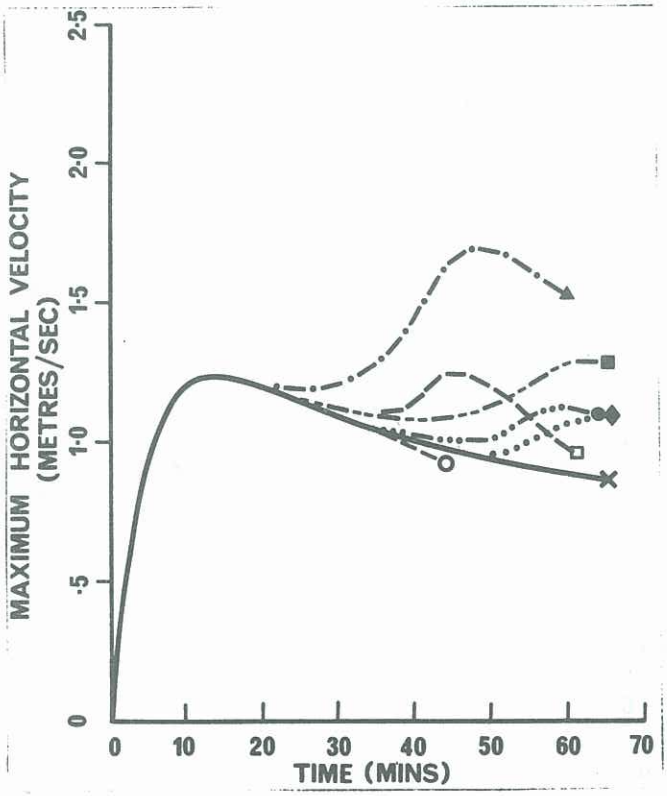

Figure 7: maximum horizontal velocity as a function of time, code as for figure 3.

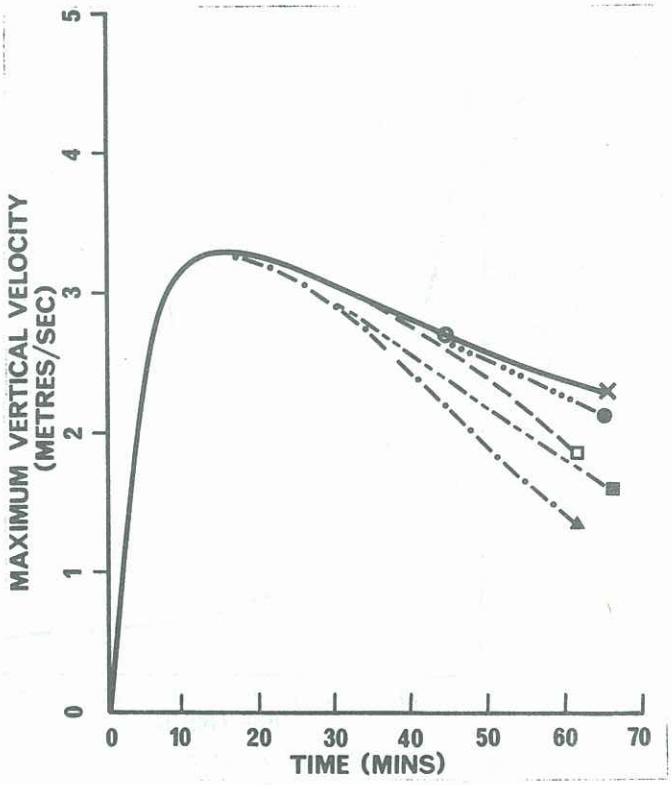

Figure 8: maximum vertical velocity as a function of time for the different boundary conditions, code as for figure 3.

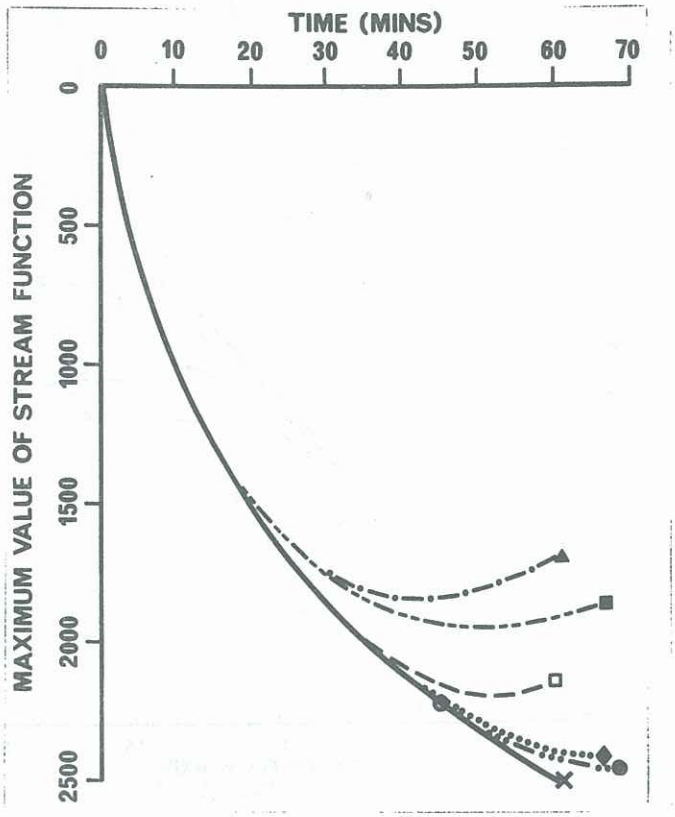

Figure 9: maximum value of the stream function for the different boundary conditions. Pseudo Rayleigh Number 3. Code as for figure 3.

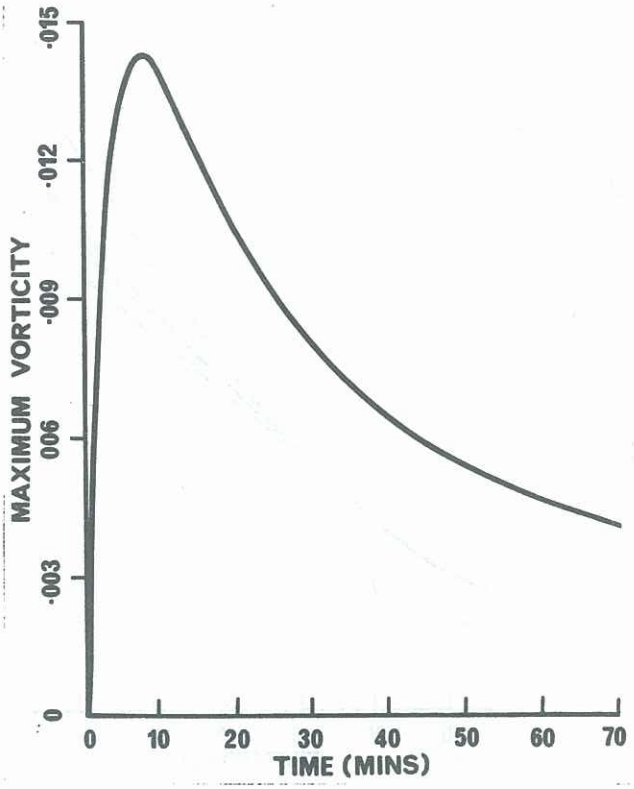

Figure 10: maximum vorticity as a function of time. Pseudo Rayleigh Number 3. All experiments lie on the same graph.

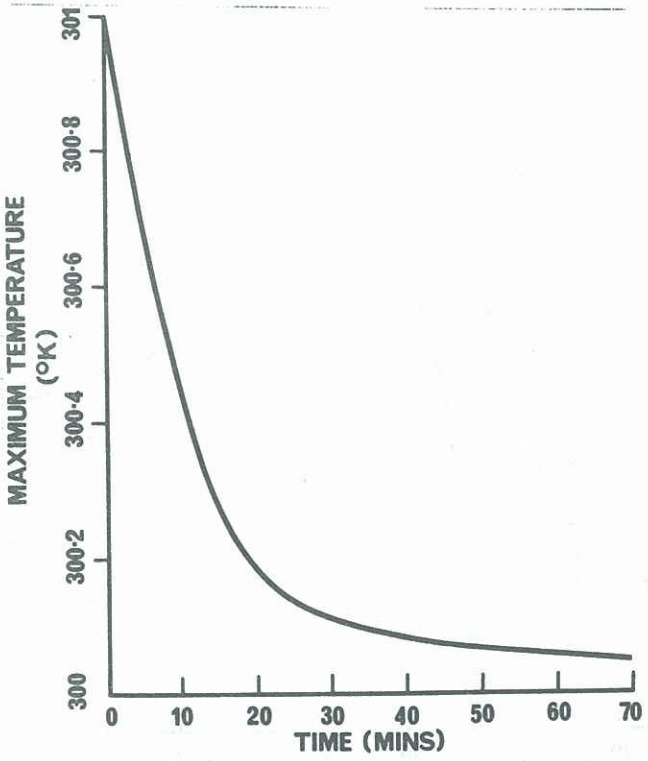

Figure 11: maximum temperature as a function of time. Pseudo Rayleigh Number is 3. All experiments lie on the same graph.